Research Article

Journal of Applied Toxicology

Received: 30 November 2011, Revised: 30 January 2012, Accepted: 30 January 2012 Published online in Wiley Online Library: 23 April 2012

(wileyonlinelibrary.com) DOI 10.1002/jat.2742

Acute toxic effects and gender-related biokinetics of silver nanoparticles following an intravenous injection in mice

Yuying Xue,[a]* Shanshan Zhang,[a] Yanmei Huang,[a] Ting Zhang,[a] Xiaorun Liu,[a] Yuanyuan Hu,[a] Zhiyong Zhang[b] and Meng Tang[a]

ABSTRACT: This study evaluated the acute toxicity and biokinetics of intravenously administered silver nanoparticles (AgNPs) in mice. Mice were exposed to different dosages of AgNPs (7.5, 30 or 120 mg kg^{-1}). Toxic effects were assessed via general behavior, serum biochemical parameters and histopathological observation of the mice. Biokinetics and tissue distribution of AgNPs were evaluated at a dose of 120 mg kg^{-1} in both male and female mice. Inductively coupled plasma–mass spectrometry (ICP-MS) was used to determine silver concentrations in blood and tissue samples collected at predetermined time intervals. After 2 weeks, AgNPs exerted no obvious acute toxicity in the mice. However, inflammatory reactions in lung and liver cells were induced in mice treated at the 120 mg kg^{-1} dose level. The highest silver levels were observed in the spleen, followed by liver, lungs and kidneys. The elimination half-lives and clearance of AgNPs were 15.6 h and 1.0 ml h^{-1} g^{-1} for male mice and 29.9 h and 0.8 ml h^{-1} g^{-1} for female mice. These results indicated that AgNPs could be distributed extensively to various tissues in the body, but primarily in the spleen and liver. Furthermore, there appears to be gender-related differences in the biokinetic profiles in blood and distribution in lungs and kidneys following an intravenous injection of AgNPs. The data from this study provides information on toxicity and biodistribution of AgNPs following intravenous administration in mice, which represents the worst case scenario of toxicity among all the different administration routes, and may shed light in the future use of products containing AgNPs in humans. Copyright © 2012 John Wiley & Sons, Ltd.

Keywords: silver nanoparticles; acute toxic effects; gender-related biokinetics; tissue distribution; mice

Introduction

The convergence of nanotechnology with nanomedicine has brought new hope to the therapeutic and pharmaceutical fields. Nanoparticles have been used as diagnostic imaging reagents, antimicrobial agents, transfection vectors and fluorescent labels (Ballou *et al*., 2004; Bharali *et al*., 2005; Coto-García *et al*., 2011; Kim *et al*., 2007; Lok *et al*., 2007). Despite the rapid progress and early acceptance of nanobiotechnology, the potential for adverse health effects owing to exposure at various levels in humans and the environment has not yet been established. It has been speculated that the impact of nanomaterials on humans and the environment will increase substantially in the future. Silver nanoparticles (AgNPs) are widely used in medicine, physics, material sciences and chemistry (Chen and Schluesener, 2008). It is estimated that, of the thousands of nanotechnology-based consumer products or product lines available on the market, products containing AgNPs are the largest (24%) and the fastest growing category (Woodrow Wilson International Center for Scholars, 2011). AgNPs have gained much popularity recently owing to their unique antibacterial, antiviral and anti-fungal properties (Kim *et al*., 2007; Lok *et al*., 2007). In addition, AgNPs have potential applications in the treatment of diseases that require sustained drug concentrations in the blood, specific cells or organs. For instance, AgNPs have been shown to undergo size-dependent interactions with the HIV-1 virus and inhibit its binding to the host cell *in vitro* (Elechiguerra *et al*., 2005). Also, AgNPs coated with silica and functionalized with aldehyde groups have been bio-conjugated with specific oligonucleotides for colorimetric DNA detection (Liu *et al*., 2005). Additionally, AgNPs possess remarkably strong antimicrobial activities and have been used medicinally in wound dressings, contraceptive devices, surgical instruments, medical catheters and bone prostheses (Chen and Schluesener, 2008; Samuel and Guggenbichler, 2004). More recently AgNPs have been incorporated into textiles for the manufacture of clothing and applied in the food industry to limit bacterial growth (Chau *et al*., 2007; Vigneshwaran *et al*., 2007). Therefore, exposure to AgNPs is becoming more of a reality in people's lives. In contrast to the attention paid to its applications, there is a serious lack of information concerning their biodistribution and organ accumulation as well as their potential toxicological implications once intake occurs.

*Correspondence to: Yuying Xue, Key Laboratory of Environmental Medicine and Engineering, Ministry of Education, Jiangsu Key Laboratory for Biomaterials and Devices, School of Public Health, Southeast University, No. 87 Dingjiaqiao, Nanjing 210009, China.
E-mail: yyxue@seu.edu.cn

[a]Key Laboratory of Environmental Medicine and Engineering, Ministry of Education, Jiangsu Key Laboratory for Biomaterials and Devices, School of Public Health, Southeast University, No. 87 Dingjiaqiao, Nanjing 210009, China

[b]CAS Key Laboratory of Biomedical Effects of Nanomaterials and Nanosafety, Institute of High Energy Physics, Chinese Academy of Sciences, Beijing 100049, China

Copyright © 2012 John Wiley & Sons, Ltd.

Journal of Applied Toxicology

Previously *in vitro* studies revealed that AgNPs showed cytotoxicity through reduced mitochondrial functions, increased membrane leakage, necrosis and induction of apoptosis (Braydich-Stolle *et al*., 2005; Choi *et al*., 2010; Hsin *et al*., 2008; Hussain *et al*., 2005; Kvitek *et al*., 2009; Lanone *et al*., 2009; Miura and Shinohara, 2009). However, there is no direct correlation of biological markers of toxicity between *in vivo* and *in vitro* studies owing to the complexity of dose delivery, mono- vs co-cultures, endpoint evaluations as well as other factors of cellular interaction with different biological media (Sayes *et al*., 2007; Seagrave *et al*., 2005). Most of the *in vivo* studies on AgNPs have employed routes of administration such as inhalation, intratracheal instillation or oral gavage (Ji *et al*., 2007; Kim *et al*., 2008; Park *et al*., 2011; Takenaka *et al*., 2001). These studies revealed that AgNPs could distribute from the exposure site and become systemically available. When nanoparticles enter the body, whether following pulmonary, dermal or oral exposure, they may become systemically available and induce potential toxicity to all organs and tissues affected. Intravenous route of administration not only allows for avoidance of variability in absorption from the absorption sites, but also represents a potential exposure route of AgNPs for their medical and diagnostic applications. Studies on the biokinetics of nanoparticles could provide relevant information for evaluation of test results from other toxicological studies and for the extrapolation of data from animals to humans.

For this purpose, mice were treated intravenously with a single injection of a suspension of AgNPs in saline at three dose levels determined during preliminary toxicity studies, and toxic effects were investigated for a period of 2 weeks. The concentration of AgNPs was determined by inductively coupled plasma–mass spectrometry (ICP-MS). Toxic effects were assessed by general behavior, serum biochemical parameters and histopathological observation. Meanwhile, biokinetics and tissue distribution were evaluated in both female and male mice at predetermined time intervals. The kinetic parameters were evaluated using computer software [Drug and Statistical Software (DAS), Version 2.1.1, Mathematical Pharmacology Professional Committee of China, Shanghai, China] after exposure to AgNPs intravenously.

Materials and Methods

Nanoparticles

Silver nanoparticles (Shanghai Huzheng Nano Technology Co. Ltd, Shanghai, China) with a manufacturer's stated average particle size of 15 nm (12–20 nm) were obtained in powder form and used as received. The intended use of this product is for its antibacterial and anti-inflammatory effect in the treatment of burns and other inflammations.

The AgNPs were characterized using a transmission electron microscope (TEM, JEM-2100, Jeol, Japan) and a scanning electron microscope (SEM, S4800, Hitachi, Japan). Upon dispersing the AgNPs particles in saline and prior to intravenous injection into animals, the particle size distribution of AgNPs in the suspension was measured with a laser diffraction particle size analyzer (Zetasizer Nano-ZS90, Malvern, UK).

Animals

The experimental protocols were approved by Southeast University Faculty of Medicine Animal Experimental Committee. ICR mice of either sex (provided by Qinglongshan Experimental Animal Center, Nanjing, China), aged 5 weeks, were used in the experiments. Five mice of the same sex were housed in a stainless steel cage containing sterile paddy husk as bedding in ventilated animal rooms. They were acclimated in the controlled environment (temperature $22 \pm 2\,^{\circ}C$; humidity $60 \pm 10\%$; and light 12 h light–dark cycle) with free access to water and a standard pellet diet *ad libitum*. The animals were acclimated to the environment for a week prior to dosing. All the animal experiments were performed in compliance with the local ethics committee. All experimental procedures conformed to the guide for the care and use of laboratory animals (National Research Council, 1996).

Investigation of General Toxicology

Forty-eight mice were randomly divided into four groups, a control group and three experimental groups, with six male and six female mice in each group. The animals were treated with either saline (control group) or AgNPs suspension at concentrations of 0.75, 3.0 and 12.0 mg ml^{-1}. Prior to dosing, AgNPs suspensions were prepared in saline at the concentrations mentioned above. The suspensions were vortexed vigorously for 5 min and sonicated for 45 s to ensure uniformity. Mice were injected via a tail vein with saline or the test suspensions at a volume of 10 µl g^{-1} body weight [b.w.; doses of 7.5 (low-dose), 30 (mid-dose) and 120 (high-dose) mg kg^{-1} b.w.]. Currently, there is a lack of clinical or environmental dose information for human exposure. The experimental doses were selected based on the results of a preliminary study where a lethal dose of >200 mg kg^{-1} b.w. was observed. Immediately after dosing, the vital signs and toxic effects of mice in each group were recorded. The body weight of each animal was measured at the initiation of treatment, then once a week during the treatment period thereafter. Half of the mice in each group were killed on day 7 and the remaining mice were killed on day 14 following treatment. Weights of organs (heart, lungs, liver, spleen and kidneys) were taken and relative organ weights were calculated based on body weight. Blood and tissue samples were collected for hematological examination and histopathological studies.

Serum Biochemistry

Mice were killed by exsanguination under ether anesthesia at day 7 or 14 post-injection. Before necropsy about 1 ml of blood was drawn by removing the right eyeball and allowed to clot for biochemical analyses of serum. Serum biochemical parameters, including albumin (ALB), alkaline phosphatase (ALP), blood urea nitrogen (BUN), creatinine (CRE), glutamic oxalacetic transaminase (GOT), glutamic pyruvic transaminase (GPT), lactate dehydrogenase (LDH), total cholesterol (T-CHO) and total protein (TP), were analyzed using a biochemical blood analyzer (Hitachi 7150, Hitachi, Japan).

Histopathology

After the blood was collected, the mice were killed by cervical dislocation. The brain, heart, lungs, liver, spleen, kidneys, testicle or ovary were then carefully removed by incision. The organs

 Copyright © 2012 John Wiley & Sons, Ltd.

were then fixed in a 10% formalin solution containing neutral phosphate-buffered saline. The tissues were routinely processed, embedded in paraffin, sectioned at 3–5 μm, and then stained with haematoxylin and eosin for microscopic examination.

Biokinetics and Tissue Distribution

To study the kinetics and tissue distribution of AgNPs in mice, 100 ICR mice (b.w. 24–26 g) were used and divided into ten groups in a random manner, with five males and five females in each group. For the biokinetics study, mice were given a 12 mg ml^{-1} AgNPs suspension at a volume of 10 μl g^{-1} b.w. via tail vein injection. This dose was chosen because (1) it is low enough to be acutely nontoxic based on the observation of the acute toxic effects; and (2) it is high enough to allow quantification of silver residue levels in organs of interest at later time points. The AgNPs powder was dispersed in saline, then vortexed vigorously for 5 min and sonicated for 45 s before injection. Blood samples (about 0.8–1.0 ml for each mouse) retrieved from the ocular vein were collected at predetermined time intervals (10, 20, 30 min and 1, 3, 6, 12, 24 h post-injection). For the tissue distribution study, mice were injected with the same dosage of AgNPs suspension as mentioned above. Animals were killed and tissues (lungs, liver, spleen and kidneys) were harvested at time points of 6, 12 h and 1, 7, 14 days following injection. In this experiment, 12 mice injected with saline at the volume of 10 μl g^{-1} b.w. were simultaneously used as negative controls. At each time point 1, 7, 14 days following injection, four mice (two male and two female) were killed and tissues were collected. All the blood and tissue samples were stored in a −60 °C refrigerator for further analysis.

ICP-MS Analysis

The silver analysis was based on the quantification of ^{107}Ag in various samples using an inductively coupled plasma–mass spectrometry (ICP-MS) method. Blood and tissue samples were taken out and thawed. About 40–80 mg of each sample was weighed, digested and analyzed for silver content. In brief, prior to the elemental analysis, the blood and tissue samples of interest were digested in 5 ml nitric acid (ultrapure grade) overnight. After adding 1 ml hydrogen peroxide (H_2O_2, 30% v/v, MOS grade), the mixtures were heated at about 200 °C using an electrical heat plate until the digestion were complete, as indicated by being free of particulates and color in the solution. The solution (about 1 ml) was diluted to a total volume of 10 ml with 2% nitric acid. ICP-MS (Thermo Elemental X7, Thermo Electron Co., USA) was used to analyze the silver concentration in the samples. Calibration plots of standards of ^{107}Ag were obtained by injecting a series of standard solutions (0.1, 0.5, 1, 5, 10, 50 ng ml^{-1} in 2% nitric acid). To ensure the accuracy and precision of the technique, the standard of indium solution was added online as an internal standard element. The detection limit of silver was 0.001 ng ml^{-1}. Data are expressed as micrograms per gram of fresh blood or tissue.

Statistical Analysis

The quantitative data were expressed as means ± standard deviation. A multiple variance analysis and Duncan's multiple range tests were performed to compare the relative organ weights, and results of the blood biochemistry between the three experimental groups and the control mice. The software used for the data analysis was SPSS 13.0 for Windows (SPSS Inc., Chicago, IL, USA). The time-course changes in blood silver levels between male and female mice were compared by repeated measure ANOVA. Incidence data were compared by chi-square analysis. *P*-Values of less than 0.05 were considered significant. The biokinetic analysis was performed with DAS using a noncompartmental modeling approach. The biokinetic parameters were calculated using standard equations including area under the curve (AUC), steady state volume of distribution (V_{dss}), elimination half-life ($T_{1/2}$), mean residence time (MRT), and clearance (*Cl*).

Results

Particle Characterization

Particles were reported by the manufacturer to be approximately 15 nm in diameter. TEM was used to measure the primary particle size of more than 400 random particles and compare the average with manufacturer's specifications. As shown in the TEM images (Fig. 1A, B), the silver particles were uniform in size and shape. Particles with diameter ranging from 10 to 30 nm accounted for 96% of the total particle count, with an average diameter of 21.8 nm. Furthermore, the SEM image (Fig. 1C) showed the silver particles to have good dispersion. However, as measured by laser diffraction particle analyzer at the time of injection, silver particles suspended in saline were 3.1–117 nm in diameter with a peak maximum at 90.5 nm accounting for 91% of the total particle count (Fig. 1D). The results of particle characterization show that mice were exposed to agglomerates of AgNPs that were larger than the primary nanoparticles.

General Effects of Toxicity and Gross Observation

Upon administration of AgNPs, no abnormal behavior or clinical symptoms were observed in the experimental animals. At necropsy, discolored lungs, darkened liver and slight edema were visually observed in 2/6 mice on day 7 and in 3/6 mice on day 14 for the high-dose group. The other organs looked normal in all experimental animals. No significant changes in body weights and relative organ weights of the animals were observed throughout the study period (Table 1).

Serum Biochemistry

After 7 days of treatment, a statistically significant increase in the LDH level was observed in the low-dose group when compared with the control group. After 7 days of exposure to AgNPs, a statistically significant decrease in the TP and ALB levels was noted in the low-dose and the mid-dose groups when compared with the control group. On day 14, the mid-dose group exhibited significantly higher LDH and BUN levels than those in the control group. The low dose group displayed a GOT level that was significantly lower than that of the control group. The other serum biochemical parameters such as GPT, ALP, CRE and T-CHO did not show significant differences between the treatment and the control groups (Table 2). Neither were there any significant dose-related changes in serum biochemistry

Copyright © 2012 John Wiley & Sons, Ltd.

Journal of Applied Toxicology

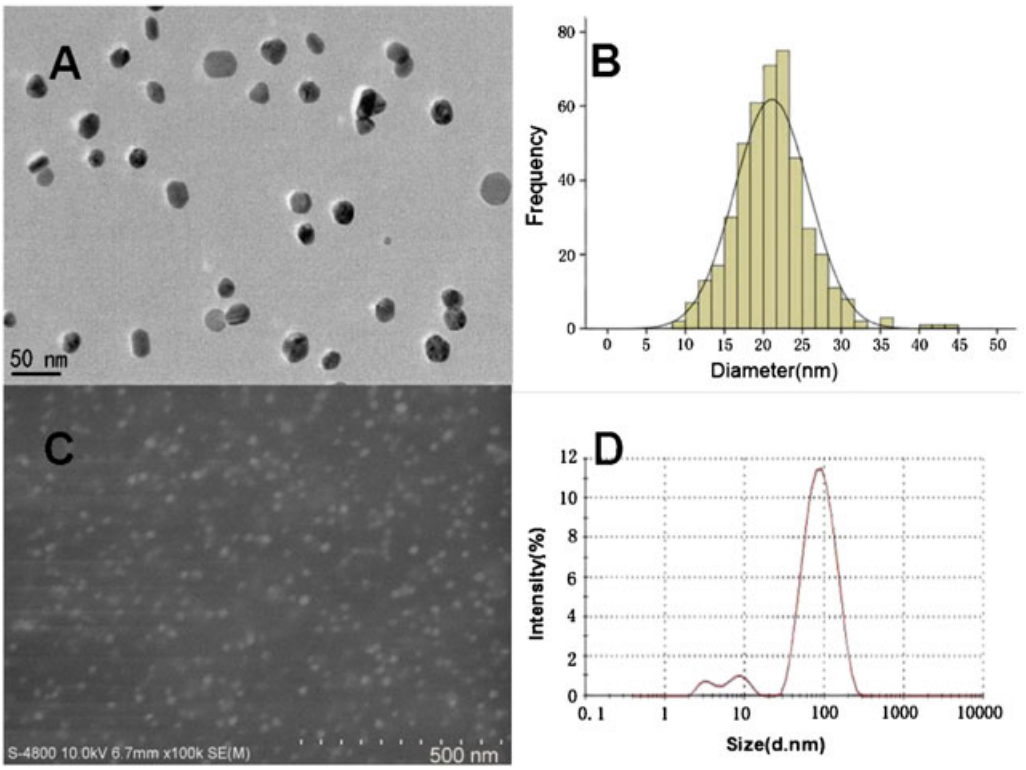

Figure 1. Characteristics of silver nanoparticles: (A) transmission electron micrograph of silver nanoparticles. Bar indicates 50 nm. (B) The size distribution histogram generated using image (A) showing nanoparticles of size 10–30 nm with an average diameter of 21.8 nm. (C) Scanning electron micrograph of silver nanoparticles showed well-dispersed particles. (D) Particle size distribution of AgNPs in saline suspension used for intravenous injection showing particles of diameter ranging from 3.1 to 117 nm, with a peak of distribution at 90.5 nm. The results indicate the presence of silver nanoparticle agglomerates in saline.

parameters. Some parameters showed relatively large standard deviations, which could be due to inter-animal variation.

Histopathology

Histopathological observations of tissues were conducted (Fig. 2). Lungs from high-dose AgNPs exposure demonstrated thickened alveolar walls and infiltration of focal inflammatory cells on day 7, but these changes diminished by day 14. Slight interstitial edema and infiltration of inflammatory cells were observed in lungs in the mid-dose group, compared with slight and negligible changes in the control group. Edema and loose cytoplasm on liver cells were found in the high-dose AgNPs treatment mice. No infiltration of inflammatory cells was present on liver cells in all mice. There were no remarkable histopathological changes in brain, heart, spleen, kidneys, testicles or ovaries in all of the experimental animals.

Table 1. Body weights and relative organ weights following intravenous exposure to AgNPs in mice (n = 6)

Dose (mg/kg)	Body weight, g (before treatment)	Body weight, g (after treatment)	Heart	Lungs	Liver	Spleen	Kidneys
			7 days				
Saline(control)	25.33 ± 2.58	31.33 ± 5.00	0.46 ± 0.03	0.63 ± 0.22	6.80 ± 0.53	0.58 ± 0.10	1.17 ± 0.14
7.5	24.83 ± 3.87	29.33 ± 3.27	0.44 ± 0.08	0.63 ± 0.11	6.92 ± 0.79	0.63 ± 0.17	1.27 ± 0.15
30	25.33 ± 1.86	29.83 ± 3.49	0.42 ± 0.03	0.61 ± 0.09	6.84 ± 0.64	0.56 ± 0.05	1.23 ± 0.14
120	24.00 ± 1.09	27.67 ± 5.32	0.40 ± 0.04	0.70 ± 0.43	6.68 ± 0.69	0.66 ± 0.16	1.10 ± 0.08
			14 days				
Saline(control)	26.00 ± 1.67	27.56 ± 4.46	0.45 ± 0.62	0.76 ± 0.17	5.83 ± 0.32	0.65 ± 0.96	1.39 ± 0.15
7.5	25.00 ± 2.53	29.74 ± 5.89	0.46 ± 0.31	0.69 ± 0.17	5.55 ± 0.26	0.57 ± 0.11	1.40 ± 0.17
30	26.00 ± 1.26	32.17 ± 7.65	0.45 ± 0.55	0.82 ± 0.14	6.19 ± 0.80	0.62 ± 0.12	1.38 ± 0.28
120	24.67 ± 1.37	28.28 ± 4.76	0.46 ± 0.55	0.66 ± 0.21	5.94 ± 0.58	0.57 ± 0.11	1.37 ± 0.26

Data are expressed as means ± standard deviation. Relative organ weights (%) were calculated as wet organ weight based on the body weight. No significant difference was observed between the experimental group and the control group.

 Copyright © 2012 John Wiley & Sons, Ltd.

Table 2. Serum biochemical parameters following intravenous exposure to AgNPs in mice ($n = 6$)

Biochemical parameters		Experimental group (mg/kg)			Control
		7.5	30	120	(saline)
7 days	ALB (g l^{-1})	13.83 ± 1.47*	13.33 ± 1.03*	15.92 ± 0.92	16.17 ± 1.83
	ALP (IU l^{-1})	315.33 ± 95.48	350.33 ± 116.61	254.20 ± 32.84	275.50 ± 106.13
	BUN (mmol l^{-1})	8.38 ± 1.41	8.03 ± 1.53	8.95 ± 2.17	8.30 ± 1.40
	CRE (μmol l^{-1})	46.00 ± 8.05	45.17 ± 6.79	41.80 ± 5.19	41.00 ± 4.78
	GOT (IU l^{-1})	93.00 ± 7.64	98.50 ± 8.46	165.80 ± 128.15	93.17 ± 6.31
	GPT (IU l^{-1})	43.67 ± 10.15	44.33 ± 8.85	82.80 ± 87.13	38.17 ± 5.85
	LDH (IU l^{-1})	789.00 ± 341.03*	575.33 ± 65.70	640.20 ± 53.30	429.33 ± 44.00
	T-CHO (mmol l^{-1})	2.63 ± 0.71	3.22 ± 0.64	3.04 ± 0.52	3.02 ± 0.47
	TP (g l^{-1})	50.17 ± 4.71*	48.67 ± 3.61*	55.33 ± 2.66	55.33 ± 3.78
14 days	ALB (g l^{-1})	14.50 ± 2.43	14.50 ± 3.51	14.83 ± 1.17	15.17 ± 1.47
	ALP (IU l^{-1})	148.00 ± 15.17	202.33 ± 88.93	243.83 ± 113.09	190.00 ± 67.75
	BUN (mmol l^{-1})	7.28 ± 1.25	8.93 ± 1.03*	7.67 ± 1.74	6.55 ± 1.67
	CRE (μmol l^{-1})	34.00 ± 4.00	39.17 ± 4.02	36.50 ± 5.05	34.17 ± 6.31
	GOT (IU l^{-1})	100.00 ± 17.19*	139.00 ± 34.88	129.33 ± 20.89	131.00 ± 17.65
	GPT (IU l^{-1})	44.67 ± 16.90	62.83 ± 47.76	60.83 ± 34.91	55.17 ± 11.70
	LDH (IU l^{-1})	555.67 ± 122.11	667.00 ± 217.24*	536.00 ± 77.24	464.17 ± 123.79
	T-CHO (mmol l^{-1})	2.94 ± 0.78	2.97 ± 0.64	2.94 ± 0.38	2.80 ± 0.79
	TP (g l^{-1})	55.17 ± 3.87	55.33 ± 3.88	56.00 ± 4.15	56.83 ± 3.19

Data are expressed as means ± standard deviation.
* Significant difference from the control value, $P < 0.05$.
ALB, Albumin; ALP, alkaline phosphatase; BUN, blood urea nitrogen; CRE, creatinine; GOT, glutamic oxalacetic transaminase; GPT, glutamic pyruvic transaminase; LDH, lactate dehydrogenase; T-CHO, total cholesterol; TP, total protein.

Biokinetics of AgNPs in Blood

Blood silver concentrations as a function of time following an intravenous injection are shown in Fig. 3. Silver levels in blood were observed to fall rapidly for both male and female mice after dosing, and a valley concentration was found at 1 h after injection. The blood silver levels persisted and increased slightly from 1 to 6 h and were then maintained at a lower level of about 2 μg g^{-1} until 24 h. Silver was not detected in any mice in the control group. Although the biological manifestations were similar for the male and female mice, the blood silver concentration profiles during the initial 24 h after dosing showed a significant difference between the male and the female mice ($P = 0.000$ when compared over 24 h by repeated measure ANOVA). The kinetic parameters estimated by noncompartmental modeling analysis using DAS are shown in Table 3. The half-lives of elimination evaluated from the curve until 24 h were 15.6 h for the male mice and 29.9 h for the female mice. Besides the two-fold difference in half-life, other kinetic parameters such as AUC, MRT and V_{dss}, were also larger for the female mice than for the male mice. However, *Cl* values were similar between the genders.

Tissue Distribution of AgNPs

To investigate the tissue distribution and disposition of AgNPs following an intravenous injection in mice, the concentrations of silver in lungs, liver, spleen and kidneys at various experimental time points were determined by ICP-MS method. Mean values comparing male with female mice are plotted in Fig. 4 and listed in Table 4. No silver was detected in the organs of mice in the control group. After a single intravenous dose of 120 mg kg^{-1}, the silver levels were highest in the spleen, followed in a decreasing order by liver, lungs and kidneys. The silver was retained in the spleen for the entire duration of the experiment, especially for the female mice, with an average level of silver of 186.8 μg g^{-1} on day 1 and 180.6 μg g^{-1} on day 14. After 1 day of exposure, the concentration of silver in the spleen was almost 10 times that in the lungs and about 90 times the amount in the kidneys for the female mice, and almost 8 times that in the lungs and about 60 times the amount in the kidneys for the male mice. In the liver, the silver levels were steady at about 120 μg g^{-1} on the first day, and showed a slightly decreasing trend in silver levels from day 1 to days 7 and 14. In the lungs, the results were variable during the first day, and showed a decrease in silver levels from day 1 to day 7, but a slight increase from day 7 to day 14. Similarly, in the kidneys, there was a slight increase in silver levels on day 14, although the levels of silver were maintained at a low level during the 14-day experimental period. In addition, the lungs and kidneys showed a gender-dependent accumulation of silver, with significantly higher levels of silver in the female mice when compared with the male mice following the 14-day administration.

Discussion

Silver has been used as an antimicrobial agent for a long time (Monteiro *et al.*, 2009). Over the last couple of decades, silver has been engineered into nanoparticles with dimensions ranging from 1 to 100 nm. Silver nanoparticles have recently gained interest for a range of biomedical applications, owing to their potent antibacterial activity (Chen and Schluesener, 2008; Salata, 2004). It is estimated that, of the nanomaterials in

Copyright © 2012 John Wiley & Sons, Ltd.

Journal of Applied Toxicology

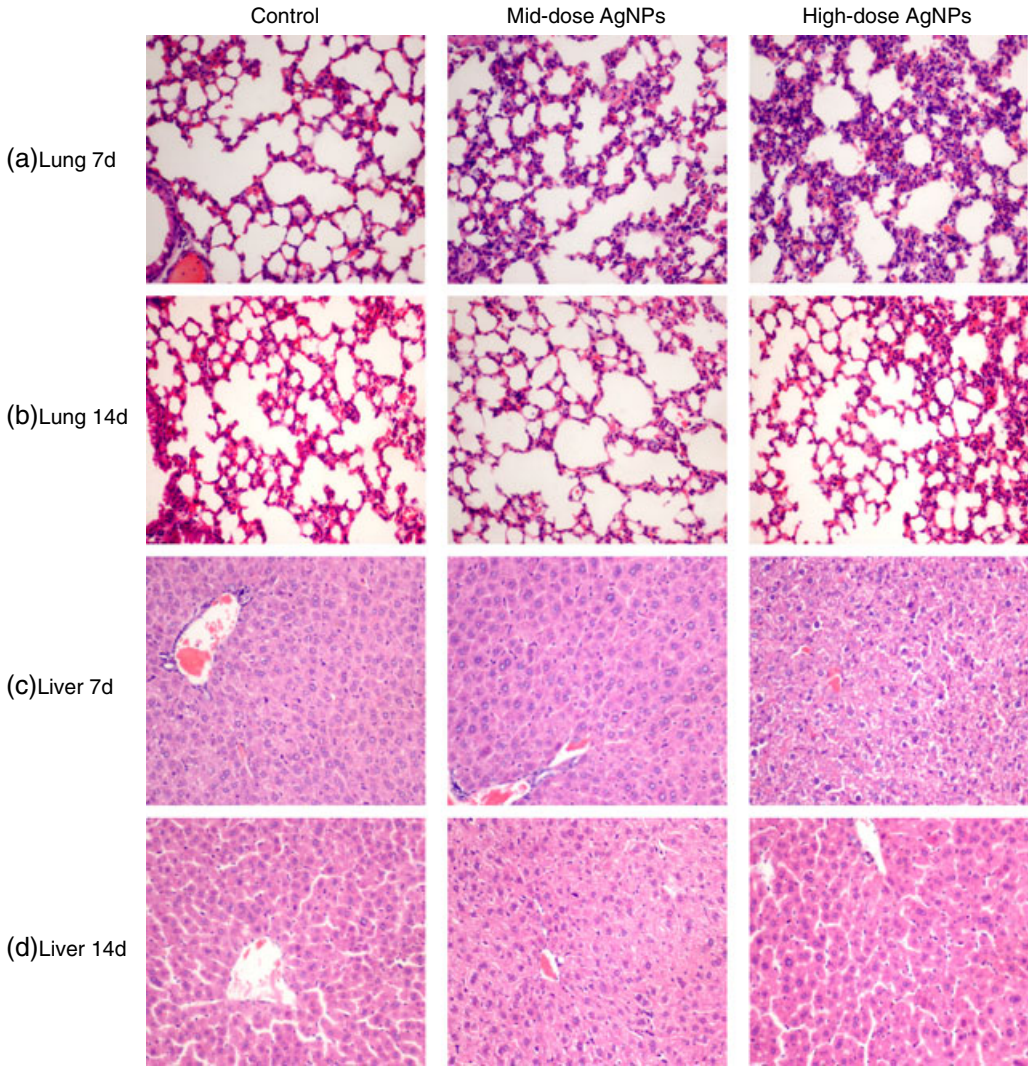

Figure 2. The histopathological changes following intravenous injection of saline (control), 30 mg kg^{-1} (mid-dose) silver nanoparticles (AgNPs) and 120 mg kg^{-1} (high-dose) AgNPs (200×). Hematoxylin and eosin stains of lung at 7 days (a) and 14 days (b); and liver at 7 days (c) and 14 days (d) after exposure.

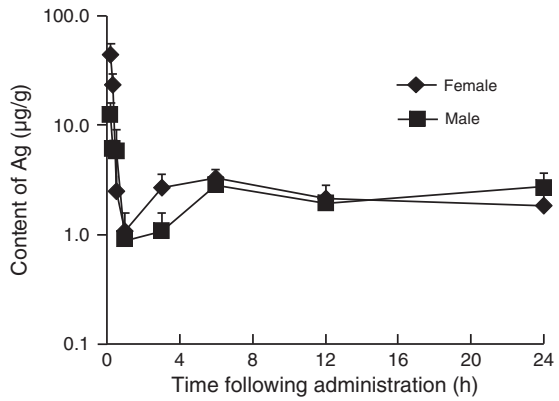

Figure 3. The blood concentration of silver as a function of time in mice. AgNPs were injected into mice via a tail vein at a dose of 120 mg kg^{-1}. Ten mice, five female and five male, were used at each time point. Data are expressed as means ± standard deviation ($n = 5$). A significant difference in the blood silver levels was observed between female and male mice ($P = 0.000$ when compared over 24 h by repeated-measure ANOVA).

Table 3. Kinetic parameters of silver nanoparticles in the mice following a dose of 120 mg kg^{-1} via intravenous injection

Parameter	Female ($n = 5$)	Male ($n = 5$)
AUC (μg ml^{-1} h^{-1})	163.9	127.0
$T_{1/2}$ (h)	29.9	15.6
MRT (h)	36.1	31.2
Cl (ml h^{-1} g^{-1})	0.8	1.0
V_{dss} (ml g^{-1})	31.9	21.7

The kinetic parameters were estimated by noncompartmental modeling analysis using Drug and Statistical Software (DAS 2.1.1). Data were determined based on the average levels at various experimental time points from individual female ($n = 5$) or male ($n = 5$) mice, so no standard deviation can be shown for parameters. AUC, Area under blood levels extrapolated to infinity; $T_{1/2}$, elimination half-life; MRT, mean residence time; *Cl*, clearance; V_{dss}, volume of distribution under a steady-state condition of blood levels.

 Copyright © 2012 John Wiley & Sons, Ltd.

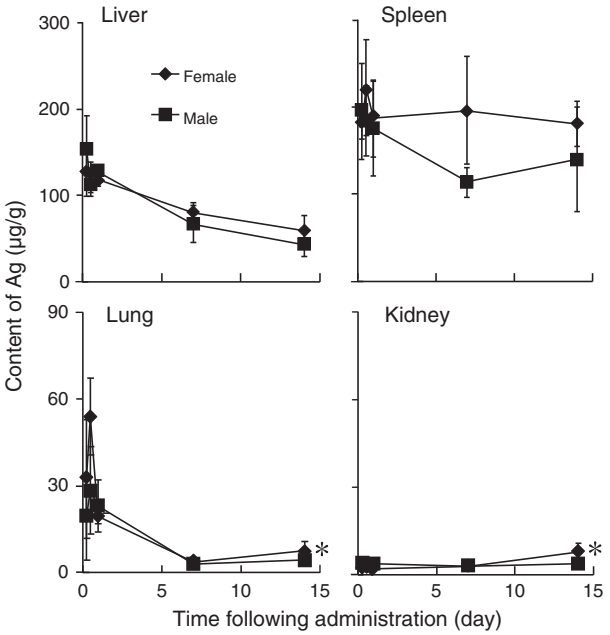

Figure 4. Tissue concentration of silve as a function of time in mice. AgNPs were injected into mice via a tail vein at a dose of 120 mg kg^{-1}. Ten mice, five female and five male, were used at each time point. Data are expressed as means ± standard deviation ($n = 5$). * $P < 0.05$ when silver levels between female and male mice were compared.

the medical and healthcare sectors, application of AgNPs has the highest degree of commercialization (Woodrow Wilson International Center for Scholars, 2011). AgNPs have gained increasing access to tissues, cells and biological molecules within the human body (Xue and Tang, 2009). From previous *in vitro* studies, AgNPs have been found to induce cytotoxicity and genotoxicity in human cells (Ahamed *et al.*, 2008; AshaRani *et al.*, 2009). However, the implications of such *in vitro* toxicity are not clear and no *in vivo* toxicity studies on AgNPs have been reported so far. Regarding the biodistribution of AgNPs, most studies reported so far have employed administration routes such as inhalation, gastric lavage and transdermal delivery (Chen *et al.*, 2009; Ji *et al.*, 2007; Kim *et al.*, 2008; Park *et al.*, 2011; Stebounova *et al.*, 2011; Sung *et al.*, 2008; Takenaka *et al.*, 2001). Very few studies have been conducted to elucidate the biokinetics of AgNPs in the body. Once nanoparticles enter the body, they may become systemically available regardless of administration route, and owing to their extremely small particle size, they may be retained in organs and cause toxic effects. For nanoparticles of medical applications, their efficacy largely depends on the control of their distribution within the body. This makes it important to illustrate the concentration–time profiles in the blood and tissues of interest. The aim of the present study was to assess the potential toxicity of AgNPs when given intravenously to mice at different doses, and to monitor biokinetics and tissue distribution following a single intravenous injection of AgNPs in mice of both genders.

The results from the acute toxicity evaluation in this study indicate that mice exposed to AgNPs by a route that allowed immediate and complete systemic availability (i.e. intravenous administration) exhibited few toxic or adverse health effects. Only mild histopathological changes were observed in the lungs and liver, when the high dose of 120 mg kg^{-1} b.w. was administered. In our preliminary studies, mice died within 30 h when injected intravenously at a dose level of 200 mg kg^{-1}. Edema in lungs and liver was observed in autopsy immediately after death. This result is similar to that reported by Kim *et al.* (2008), who studied silver nanoparticles (60 nm) administered to Sprague–Dawley rats following a 28-day oral administration at a much larger dose of 1000 mg kg^{-1} per day. As in our studies, these researchers reported no significant changes in body weight relative to the doses of silver nanoparticles during the 28-day experiment. Their study also indicated slight liver damage upon exposure to more than 300 mg of silver nanoparticles. The results suggested that AgNPs could be well tolerated in mice when given intravenously at the dose level of 120 mg kg^{-1} body weight.

Reports on *in vivo* biokinetic properties of AgNPs are sparse. The present study, by the nature of its design, provides an accurate assessment of the disposition of AgNPs in mice. The use of the intravenous route of administration avoids confounding factors associated with drug absorption by oral or other extravascular routes of administration. Silver levels in blood dropped rapidly after the intravenous bolus dosing, and a valley

Table 4. The silver levels in tissues in male and female mice following an intravenous injection

Mice	The time sampled	Concentrations of Ag (μg g^{-1})			
		Liver	Spleen	Lung	Kidney
Female ($n = 5$)	6 h	124.08 ± 24.61	178.93 ± 16.07	32.35 ± 20.61	2.61 ± 0.81
	12 h	120.92 ± 17.67	221.83 ± 55.07	54.03 ± 13.42	2.77 ± 1.17
	1 day	118.39 ± 7.00	186.83 ± 44.32	19.62 ± 2.83	2.68 ± 0.39
	7 days	80.54 ± 11.12	195.57 ± 61.81	3.73 ± 1.22	2.92 ± 0.66
	14 days	58.49 ± 18.53	180.60 ± 25.73	7.67 ± 3.10*	8.01 ± 2.96*
Male ($n = 5$)	6 h	154.41 ± 37.77	195.08 ± 55.24	19.12 ± 14.66	3.51 ± 1.26
	12 h	110.86 ± 11.36	183.98 ± 39.84	28.31 ± 15.08	2.98 ± 1.14
	1 day	126.55 ± 3.82	175.45 ± 54.61	23.02 ± 8.86	3.65 ± 0.76
	7 days	67.23 ± 20.95	113.73 ± 16.82	2.87 ± 0.62	2.74 ± 0.60
	14 days	43.07 ± 14.19	139.90 ± 59.43	4.21 ± 1.18	3.84 ± 1.69

The dose of AgNPs injected via a tail vein was 120 mg kg^{-1} body weight. Data are expressed as means ± standard deviation ($n = 5$). * $P < 0.05$ compared with corresponding silver levels between female and male mice.

Copyright © 2012 John Wiley & Sons, Ltd.

Journal of AppliedToxicology

concentration was observed 1 h after dosing. The blood silver levels were slightly increased between 1 and 6 h and then maintained at lower levels afterwards. The concentration–time profile of intravenously administered AgNPs showed that AgNPs could be transported rapidly to various organs within 1 h. Redisposition appears to occur after 1 h, and an equilibrium of distribution would be achieved after 6 h as a result of systemic blood circulation. These results are comparable to the recent report by Lankveld *et al*. (2010). These researchers investigated the blood kinetics and tissue distribution of different sizes of AgNPs (20, 80 and 110 nm) in rats following intravenous injection. Following a single or repeated injection, the blood silver concentration showed a rapid decline during the first 10 min, and then decreased gradually until 60 min, independent of nanoparticle size. They developed a physiologically based pharmacokinetic model to estimate the model parameters, which indicated no clear correlation between the parameters and particle size. The present study was limited to one size of AgNPs, which was complicated by the formation of agglomerates in the injected suspension. However, the agglomerates are also of nano dimension, making this study relevant to the other studies that examine the biokinetic behavior of AgNPs. It is worth pointing out that the values of kinetic parameters in the current study should not be compared with parameters in the other studies since different mathematical models and animals were used. The elimination half-lives of AgNPs in mice (29.9 h for female and 15.6 h for male mice) were long and suggested that AgNPs cannot be cleared from the body quickly. Possible explanations for the relatively slow elimination could be as follows: (a) formation of a silver–protein complex with sulfydryl-containing proteins, including metal-specific binding proteins, may occur, as silver has been known to have a high affinity to sulfur (Bell and Kramer, 1999); and (b) relatively insoluble particles of AgNPs may be involved. We determined the dissolution of AgNPs in saline and the results showed that the concentrations of silver ion in the test suspensions were very low (<0.001%). However, whether or not the degree of ionization may change under physiological conditions remains to be determined. Long blood half-life can be advantageous in the application of therapeutic agents in thermal therapy and gene/drug delivery. The volume of distribution of AgNPs in mice (31.9 ml g^{-1} for female and 21.7 ml g^{-1} for male mice) was much larger than the total body fluid of the animal (maximum 15 ml for a 25 g mouse), which suggests that distribution of AgNPs may not be limited to the extracellular fluid compartment, but rather include most organ tissues. The results of tissue distribution from the current study, as well as from studies by others on distribution, have confirmed the extensive disposition of AgNPs in the body (Chen *et al*., 2009; Ji *et al*., 2007; Kim *et al*., 2008; Loeschner *et al*., 2011; Park *et al*., 2011; Stebounova *et al*., 2011; Sung *et al*., 2008; Takenaka *et al*., 2001). The huge V_{dss} in mice is consistent with data from the earlier nanoparticle kinetic study for CdSeS quantum dots (21.3 ± 2.0 nm in diameter, $V_d = 1611 \pm 112$ ml kg^{-1}; Chen *et al*., 2008) that also demonstrated that nanoparticles might accumulate in organ tissues.

Determination of silver concentrations in various organs revealed that silver nanoparticles mainly accumulated in the spleen, liver, lungs and kidneys, but rarely distributed in the brain, heart, muscle, adipose and spermary/ovary, since silver levels in these organs were detected to be under 1 μg g^{-1} at different time points in our preliminary experiment (data not shown). Silver particles were primarily concentrated in the spleen, followed by liver, lungs and kidneys. The results are in agreement with previous reports describing distribution of AgNPs to multiple tissues including brain, lungs, liver, stomach, kidneys, testes and skin (Chen *et al*., 2009; Ji *et al*., 2007; Kim *et al*., 2008; Park *et al*., 2011; Stebounova *et al*., 2011; Sung *et al*., 2008; Takenaka *et al*., 2001). Depending on the route of exposure, the highest concentrations were found in lungs, stomach, skin, liver and kidneys. By using intravenous administration, Lankveld *et al*. (2010) indicated that the 20 nm AgNPs distributed mainly to liver, followed by kidneys and spleen, whereas the larger particles (80 and 110 nm) distributed mainly to spleen followed by liver and lungs. This suggests that physicochemical properties of nanoparticles may contribute to the tissue distribution in the body. In the present study, the primary size of AgNPs was 21.8 nm. However, the particles agglomerated in saline and were determined to be 90.5 nm in diameter for injection. Discontinuous endothelium is characteristic for organs such as the liver and the spleen, with pores of 50–100 nm. It has also been noted that nanoparticles, like other particulate systems, are rapidly captured and retained by organs compromising the reticuloendothelial system (Stern and McNeil, 2008). Liver and spleen are the major targets of nanoparticle accumulation, especially after intravenous administration (Chrastina and Schnitzer, 2010). In the liver, the particles are mainly retained by the Kupffer cells, while the hepatocytes and the liver endothelial cells may play a secondary role. In the spleen, the marginal zone and the red pulp macrophages are the major scavengers, while peritoneal macrophages and dentritic cells have a minor contribution. In the present study, the spleen had high levels of silver during the 14-day experimental period. The long-term biological effects owing to sustained high level of AgNPs in the spleen need to be further studied, although no adverse effects and histopathological changes were observed in this study. The levels of silver in the liver decreased after one day, which implied that silver could be cleared by the liver. Furchner *et al*. (1968) found that, when silver was given orally, it was eliminated with bile in tissue through the liver metabolism, although AgNPs that are not cleared may be deposited in the liver for a long time, as relatively high levels were observed in the liver after the 14th day. The biological effects owing to deposited AgNPs in the liver also need to be further clarified. The results suggest that spleen and liver are the main target organs of AgNPs accumulation when administered intravenously. A further study would be needed to determine whether or not adverse biological effects would be induced by sustained high silver levels in target organs such as the liver and spleen over an extended period of time.

Furthermore, gender-related differences in biokinetic profiles in blood and distribution in the lungs and kidneys following an intravenous injection of AgNPs were observed in this study. In a 28-day oral study, Kim *et al*. (2008) found that the accumulation of silver in the kidneys was two-fold higher in female rats than that in male rats. Similar results were noted in the subchronic 90-day studies on AgNPs inhalation (Sung *et al*., 2008). The exact functional toxicity consequence is not apparent for the gender difference since no significant kidney function or histopathological changes were found. The present study suggests that accumulation of AgNPs in female mouse kidneys was not dependent on route of administration, which agrees with findings of the oral studies (Kim *et al*., 2008) and inhalation studies (Sung *et al*., 2008). However, the gender-related difference for the accumulation of silver in the lungs has not been

 Copyright © 2012 John Wiley & Sons, Ltd.

previously reported. Sex-dependent biokinetic properties may, in part, explain the gender difference of accumulation of silver in kidneys and lungs following intravenous injection in mice. Further studies concerning specific mechanisms of the gender-related difference for the distribution of AgNPs *in vivo* are warranted.

In conclusion, toxicity of nanoparticles is dependent on concentration and duration of exposure, which necessitates a thorough understanding of the disposition of nanoparticles. In this study, the acute toxic effects and biokinetics of AgNPs following an intravenous injection in mice were investigated. The well-being and behavior of the animals were normal during the 14-day experimental period. Treatment with AgNPs caused changes in biochemical parameters such as TP, ALB, LDH, BUN and GOT, and induced inflammatory reactions including thickened alveolar walls and an infiltration of focal inflammatory cells in the lungs, and edema and loose cytoplasm on the liver cells in mice treated with high-dose of AgNPs. The silver levels were highest in the spleen, followed in decreasing order by the levels in the liver, lungs and kidneys. The silver levels were retained in the spleen and liver for the 14-day duration of the experiment. The half-lives of elimination and clearance of AgNPs were 15.6 h and 1.0 ml h^{-1} g^{-1} for male mice and 29.9 h and 0.8 ml h^{-1} g^{-1} for females. The results indicated that AgNPs could be distributed extensively to various tissues in the body, and the spleen and liver were the main target organs for AgNPs following intravenous administration. Furthermore, gender-related differences for the biokinetic profiles in blood and distribution in lungs and kidneys following an intravenous injection of AgNPs were observed. Data from this study will not only be useful for the toxicological evaluation of AgNPs administered by other routes in animals, but will also shed light on future toxicological evaluation in humans.

Acknowledgments

This work was supported by National Key Project on Scientific Research of China (no. 2011CB933404), National Natural Science Foundation of China (nos 30972504 and 81172697), Provincial Natural Science Foundation of Jiangsu (no. BK2011606), and Science Foundation of Southeast University (no. KJ2010440). The authors would like to acknowledge Dr Ping Tong from Abbott Laboratories at Chicago for her help with the manuscript.

References

Ahamed M, Karns M, Goodson M, Rowe J, Hussain SM, Schlager JJ, Hong Y. 2008. DNA damage response to different surface chemistry of silver nanoparticles in mammalian cells. *Toxicol. Appl. Pharmacol.* **233**: 404–410.

AshaRani PV, Hande MP, Valiyaveettil S. 2009. Anti-proliferative activity of silver nanoparticles. *BMC Cell Biol.* **10**: 65.

Ballou B, Lagerholm BC, Ernst LA, Bruchez MP, Waggoner AS. 2004. Noninvasive imaging of quantum dots in mice. *Bioconjug. Chem.* **15**: 79–86.

Bell RA, Kramer JR. 1999. Structural chemistry and geochemistry of silver–sulfur compounds: Critical review. *Environ. Toxicol. Chem.* **18**: 9–22.

Bharali DJ, Klejbor I, Stachowiak EK, Dutta P, Roy I, Kaur N, Bergey EJ, Prasad PN, Stachowiak MK. 2005. Organically modified silica nanoparticles: A nonviral vector for in vivo gene delivery and expression in the brain. *Proc. Natl. Acad. Sci.* **32**: 11539–11544.

Braydich-Stolle L, Hussain S, Schlager JJ, Hofmann MC. 2005. *In vitro* cytotoxicity of nanoparticles in mammalian germline stem cells. *Toxicol. Sci.* **88**: 412–419.

Chau TT, Campbell JI, Galindo CM, Van Minh Hoang N, Diep TS, Nga TT, Van Vinh Chau N, Tuan PQ, Page AL, Ochiai RL, Schultsz C, Wain J, Bhutta ZA, Parry CM, Bhattacharya SK, Dutta S, Agtini M, Dong B, Honghui Y, Anh DD, Canh do G, Naheed A, Albert MJ, Phetsouvanh R, Newton PN, Basnyat B, Arjyal A, La TT, Rang NN, Phuong le T, Van Be Bay P, Von Seidlein L, Dougan G, Clemens JD, Vinh H, Hien TT, Chinh NT, Acosta CJ, Farrar J, Dolecek C. 2007. Antimicrobial drug resistance of *Salmonella enterica* serovar typhi in Asia and molecular mechanism of reduced susceptibility to the fluoroquinolones. *Antimicrob. Agents Chemother.* **51**: 4315–4323.

Chen D, Xi T, Bai J, Wang J. 2009. Nanosilver subchronic toxicity and silver distribution in different rat tissues. *J. Clin. Rehabil. Tissue Engin. Res.* **13**: 3181–3183.

Chen X, Schluesener HJ. 2008. Nanosilver: a nanoproduct in medical application. *Toxicol. Lett.* **176**: 1–12.

Chen Z, Chen H, Meng H, Xing G, Gao X, Sun B, Shi X, Yuan H, Zhang C, Liu R, Zhao F, Zhao Y, Fang X. 2008. Bio-distribution and metabolic paths of silica coated CdSeS quantum dots. *Toxicol. Appl. Pharmacol.* **230**: 364–371.

Choi JE, Kim S, Ahn JH, Youn P, Kang JS, Park K, Yi J, Ryu DY. 2010. Induction of oxidative stress and apoptosis by silver nanoparticles in the liver of adult zebrafish. *Aquat. Toxicol.* **100**: 151–159.

Chrastina A, Schnitzer JE. 2010. Iodine-125 radiolabeling of silver nanoparticles for *in vivo* SPECT imaging. *Int. J. Nanomedicine* **5**: 653–659.

Coto-García AM, Sotelo-González E, Fernández-Argüelles MT, Pereiro R, Costa-Fernández JM, Sanz-Medel A. 2011. Nanoparticles as fluorescent labels for optical imaging and sensing in genomics and proteomics. *Anal. Bioanal. Chem.* **399**: 29–42.

Elechiguerra JL, Burt JL, Morones JR, Camacho-Bragado A, Gao X, Lara HH, Yacaman MJ. 2005. Interaction of silver nanoparticles with HIV-1. *J. Nanobiotechnology* **3**: 6.

Furchner JE, Richmond CR, Drake GA. 1968. Comparative metabolism of radionuclides in mammals – IV. Retention of sliver-110 m in the mouse, rat, monkey, and dog. *Health Phys.* **15**: 505–514.

Hsin YH, Chen CF, Huang S, Shih TS, Lai PS, Chueh PJ. 2008. The apoptotic effect of nanosilver is mediated by a ROS- and JNK-dependent mechanism involving the mitochondrial pathway in NIH3T3 cells. *Toxicol. Lett.* **179**: 130–139.

Hussain SM, Hess KL, Gearhart JM, Geiss KT, Schlager JJ. 2005. *In vitro* toxicity of nanoparticles in BRL 3A rat liver cells. *Toxicol. In Vitro* **19**: 975–983.

Ji JH, Jung JH, Kim SS, Yoon JU, Park JD, Choi BS, Chung YH, Kwon IH, Jeong J, Han BS, Shin JH, Sung JH, Sung KS, Yu IJ. 2007. Twenty-eight-day inhalation toxicity study of silver nanoparticles in Sprague–Dawley rats. *Inhal. Toxicol.* **19**: 857–871.

Kim JS, Kuk E, Yu KN, Kim JH, Park SJ, Lee HJ, Kim SH, Park YK, Park YH, Hwang CY, Kim YK, Lee YS, Jeong DH, Cho MH. 2007. Antimicrobial effects of silver nanoparticles. *Nanomedicine* **3**: 95–101.

Kim YS, Kim JS, Cho HS, Rha DS, Kim JM, Park JD, Choi BS, Lim R, Chang HK, Chung YH, Kwon IH, Jeong J, Han BS, Yu IJ. 2008. Twenty-eight-day oral toxicity, genotoxicity, and gender-related tissue distribution of silver nanoparticles in Sprague–Dawley rats. *Inhal. Toxicol.* **20**: 575–583.

Kvitek L, Vanickova M, Panacek A, Soukupova J, Dittrich M, Valentova E, Prucek R, Bancirova M, Milde D, Zborit R. 2009. Initial study on the toxicity of silver nanoparticles (NPs) against *Paramecium caudatum*. *J. Phys. Chem. C* **113**: 4296–4300.

Lankveld DPK, Oomen AG, Krystek P, Neigh A, Troost-de Joog A, Noorlander CW, Van Eijkeren JCH, Geertsma RE, De Jong WH. 2010. The kinetics of the tissue distribution of silver nanoparticles of different sizes. *Biomaterials* **31**: 8350–8361.

Lanone S, Rogerieux F, Geys J, Dupont A, Maillot-Marechal E, Boczkowski J, Lacroix G, Hoet P. 2009. Comparative toxicity of 24 manufactured nanoparticles in human alveolar epithelial and macrophage cell lines. *Part. Fibre Toxicol.* **6**: 14.

Liu Z, Liu Y, Yang H, Yang Y, Shen G, Yu R. 2005. A phenol biosensor based on immobilizing tyrosinase to modified core–shell magnetic nanoparticles supported at a carbon paste electrode. *Anal. Chim. Acta* **533**: 3–9.

Loeschner K, Hadrup N, Qvortrup K, Larsen A, Gao X, Vogel U, Mortensen A, Lam HR, Larsen EH. 2011. Distribution of silver in rats following 28 days of repeated oral exposure to silver nanoparticles or silver acetate. *Part. Fibre Toxicol.* **8**: 18.

Lok CN, Ho CM, Chen R, He QY, Yu WY, Sun H, Tam PK, Chiu JF, Che CM. 2007. Silver nanoparticles: partial oxidation and antibacterial activities. *J. Biol. Inorg. Chem.* **12**: 527–534.

Miura N, Shinohara Y. 2009. Cytotoxic effect and apoptosis induction by silver nanoparticles in HeLa cells. *Biochem. Biophys. Res. Commun.* **390**: 733–737.

Copyright © 2012 John Wiley & Sons, Ltd.

Monteiro DR, Gorup LF, Takamiya AS, Ruvollo-Filho AC, de Camargo ER, Barbosa DB. 2009. The growing importance of materials that prevent microbial adhesion: antimicrobial effect of medicaldevices containing silver. *Int. J. Antimicrob. Agents* **34**: 103–110.

National Research Council. 1996. *Guide for the Care and Use of Laboratory Animals*. National Academy Press: Washington, DC.

Park EJ, Choi K, Park K. 2011. Induction of inflammatory responses and gene expression by intratracheal instillation of silver nanoparticles in mice. *Arch. Pharm. Res.* **34**: 299–307.

Salata O. 2004. Application of nanoparticles in biology and medicine. *J. Nanobiotechnology* **2**: 1–6.

Samuel U, Guggenbichler JP. 2004. Prevention of catheter-related infections: the potential of a new nano-silver impregnated catheter. *Int. J. Antimicrob. Agents* **23**: S57–S78.

Sayes CM, Reed KL, Warheit DB. 2007. Assessing toxicity of fine and nanoparticles: Comparing in vitro measurements to *in vivo* pulmonary toxicity profiles. *Toxicol. Sci.* **97**: 163–180.

Seagrave J, McDonald JD, Mauderly JL. 2005. *In vitro* versus *in vivo* exposure to combustion emissions. *Exp. Toxicol. Pathol.* **57**: 233–238.

Stebounova LV, Adamcakova-Dodd A, Kim JS, Park H, O'Shaughnessy PT, Grassian VH, Thorne PS. 2011. Nanosilver induces minimal lung toxicity or inflammation in a subacute murine inhalation model. *Part. Fibre Toxicol.* **8**: 5.

Stern ST, McNeil SE. 2008. Nanotechnology safety concerns revisited. *Toxicol. Sci.* **101**: 4–21.

Sung JH, Ji JH, Yoon JU, Kim DS, Song MY, Jeong J, Han BS, Han JH, Chung YH, Kim J, Kim TS, Chang HK, Lee EJ, Lee JH, Yu IJ. 2008. Lung function changes in Sprague–Dawley rats after prolonged inhalation exposure to silver nanoparticles. *Inhal. Toxicol.* **20**: 567–574.

Takenaka S, Karg E, Roth C, Schulz H, Ziesenis A, Heinzmann U, Schramel P, Heyder J. 2001. Pulmonary and systemic distribution of inhaled ultrafine silver particles in rats. *Environ. Health Perspect.* **109**: 547–551.

Vigneshwaran N, Kathe AA, Varadarajan PV, Nachane RP, Balasubramanya RH. 2007. Functional finishing of cotton fabrics using silver nanoparticles. *J. Nanosci. Nanotechnol.* **7**: 1893–1897.

Woodrow Wilson International Center for Scholars. 2011. Project on Emerging Nanotechnologies, Consumer Products Inventory of Nanotechnology Products. Available from: http://www.nanotechproject.org/inventories/consumer/analysis_draft/ (accessed 24 November 2011).

Xue Y, Tang M. 2009. Research progresses in biological effects of nanosilver (in Chinese). *J. Southeast Univ. (Nat. Sci. Edn)* **39**: 1315–1320.

Copyright © 2012 John Wiley & Sons, Ltd.